Reactive & Functional Polymers 81 (2014) 14–21

Contents lists available at ScienceDirect

Reactive & Functional Polymers

journal homepage: www.elsevier.com/locate/react

Immobilization of rhodamine 6G in calcium alginate microcapsules based on aromatic–aromatic interactions with poly(sodium 4-styrenesulfonate)

Esteban Araya-Hermosilla [a], Daniel Muñoz [a], Sandra Orellana [a], Alejandro Yáñez [b], Andrés F. Olea [c], Felipe Oyarzun-Ampuero [a,d], Ignacio Moreno-Villoslada [a,*]

[a] Instituto de Ciencias Químicas, Facultad de Ciencias, Universidad Austral de Chile, Casilla 567, Valdivia, Chile
[b] Instituto de Bioquímica y Microbiología, Facultad de Ciencias, Universidad Austral de Chile, Chile
[c] Departamento de Ciencias Químicas, Facultad de Ciencias Exactas, Universidad Andrés Bello, Chile
[d] Department of Sciences and Pharmaceutical Technology, University of Chile, Chile

ARTICLE INFO

Article history:
Received 22 October 2013
Received in revised form 17 January 2014
Accepted 29 March 2014
Available online 12 April 2014

Keywords:
Aromatic–aromatic interactions
Alginate microcapsules
Dye immobilization
Aromatic polymers

ABSTRACT

Immobilization of rhodamine 6G in calcium alginate microcapsules was achieved using the polyanion bearing negatively charged aromatic groups poly(sodium 4-styrenesulfonate) as complexing agent. The immobilization of the dye by this method finds its basis on the stabilization of the dye/polymer complex by short-range aromatic–aromatic interactions, which are resistant to the cleaving effect of highly concentrated electrolytes. On the contrary, direct immobilization of the dye in the microcapsules resulted unsuccessful due to its high diffusion coefficient in the aqueous medium, and complexation with poly(sodium vinylsulfonate) did not improve the immobilization, since the corresponding complex is based on long-range electrostatic interactions, which are easily cleaved under the high ionic strength conditions of the microcapsule formation reaction. Thus, the present investigation represents a proof of concept on the use of aromatic–aromatic interactions between polyelectrolytes bearing charged aromatic rings and their aromatic counterions as a tool to achieve improved functionalities. The release of the rhodamine 6G/poly(sodium 4-styrenesulfonate) complex from the microcapsules has been investigated as a function of pH and temperature. Coating the microcapsules with chitosan allowed minimizing the release of the dye from the microcapsules.

1. Introduction

Immobilization of dyes in different materials is important in order to achieve stable properties and improved performances, such as efficient electronic transferences, good color retention, efficient photosensitization, and high photostability [1–2]. Immobilized in polysaccharide gels, they can be used to selectively interact with proteins and enzymes [3]. Immobilized dyes have been also used in biosensors for glucose determination [4] and pH sensing by dual colorimetric fiber indicators [5]. Rhodamine 6G (R6G) is a positively charged, fluorescent, low molecular-weight dye, interesting for applications such as materials staining [6], probe for the study of colloidal properties of aqueous suspensions of clays [7], development of latent fingerprints in forensics [8], and as main component in lasers [1,9].

The interaction between typical polyelectrolytes and their counterions can be explained by the counterion condensation theory of Manning [10–13]. Under the scope of this theory, counterions interact with the polyelectrolytes by means of non-site-specific long-range electrostatic interactions, producing territorial binding, and allowing the counterions moving around the polymer. However, these interactions are easily screened by the addition of electrolytes such as NaCl [14–15]. On the other hand, we have described that polyelectrolytes containing aromatic rings (called typical polyaromatic-anions) may undergo short-range aromatic–aromatic interactions with aromatic counterions, such as charged dyes, including R6G. These interactions are particularly strong when the polyelectrolyte charge is supported on the polymeric aromatic ring. This is a consequence of a combination of hydrophobic forces and short-range electrostatic interactions between the counterions and the complementary charged polymeric aromatic groups [15–16]. These short-range interactions are additional to long-range interactions, so they produce overall higher binding constants,

* Corresponding author. Tel./fax: +56 63 2293520.
E-mail address: imorenovilloslada@uach.cl (I. Moreno-Villoslada).

http://dx.doi.org/10.1016/j.reactfunctpolym.2014.03.017
1381-5148/

site-specific binding, and resistance to the cleaving effect of added electrolytes. Such is the case of the interaction between poly(sodium 4-styrenesulfonate) (PSS) and the xanthene dyes rhodamine B (RB) [16–18], methylene blue (MB) [15], and R6G [14]. Interesting features are described for the complexes formed, in addition to the resistance to the cleaving effect of the ionic strength. Ion pairs may be formed that tend to aggregate depending on the polymer to aromatic counterion ratio: a high tendency to both disperse and aggregate the dye on the polymer domain has been shown when a large excess and moderate excess of the polymer is present, respectively [14–15].

Calcium alginate microcapsules (CAM) are well-known materials [19–22] obtained upon gelation of alginate (ALG) in the presence of some divalent metal ions such as Ca^{2+}. ALG is a linear polysaccharide composed of 1,4-linked β-D-mannuronate (M) and α-L-guluronate (G) [23]. Both comonomers may be found in homopolymeric sequences forming short blocks of a specific monomer. Its ionization pH ranges from 3.4 to 4.4 depending on both the ALG type and the counterions of the carboxylate groups, which may consist of sodium, potassium, or other metal ions [24]. Interaction between the carboxylic groups of the G units in G rich ALG segments with Ca^{2+} cations has proved to induce controllable gelation, forming the so-called egg box conformation (Fig. 1), stabilizing a helical disposition of aligned ALG chains [23,25–27].

Encapsulation of molecules and other systems in CAM is easily performed by the ionotropic method, i.e., pouring an ALG solution on a Ca^{2+} solution in a controlled manner; the materials to be encapsulated may be included in one or both the ALG solution or the Ca^{2+} solution. This method of encapsulation presents several advantages: it is performed at room temperature in aqueous media, preventing the use of organic solvents; the resulting microcapsules dissolve and biodegrade at physiological conditions [28–29]; it allows controlling the porosity, therefore controlling the diffusion of the encapsulated molecules from the gel matrix. The release of the encapsulated components may be modulated by swelling and diffusion, and by erosion or degradation of the CAM. Highly hydrophilic molecules are released in water from CAM mainly by diffusion; in contrast the molecules poorly soluble in water are released predominantly by erosion mechanism [24]. The chemical interaction produced between the encapsulated molecules and the ALG carboxylic groups is also relevant for their release from the ALG matrix. Positively charged molecules show lower release rates than negative ones, due to electrostatic interactions with the negative charge of the carboxylic groups [30]. This is more notorious in the case of cationic macromolecules whose release from the CAM may be practically inhibited [31–32].

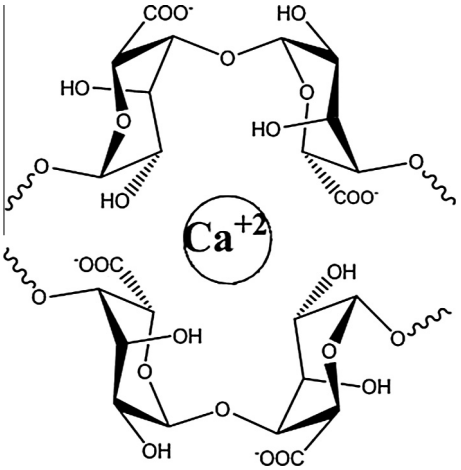

Fig. 1. Egg-box structure in CAM.

CAM are widely studied as carriers for immobilization of cells, enzymes, DNA, proteins, and other biologically important compounds. Their use for drug release control [29,33–34], stands as one of the most promising applications of the CAM, since ALG is a natural, biocompatible, nontoxic, and low cost material [33,35]. The molecules encapsulated normally present relative high size and/or hydrophobic characteristics. However, CAM have the limitation of presenting a low ability of retention of low molecular-weight, hydrophilic molecules such as dyes or several drugs, when they are exposed to a release medium or even in the microcapsule formation process, since these molecules present high diffusion coefficients in water [31]. Among hydrophilic, low molecular-weight molecules interesting to be encapsulated in CAM we find those with aromatic groups and ionizable groups in their structure. More than 75% of the drugs available in the market accomplish these requisites [36]. Many fluorescent dyes such as R6G do also present large conjugated systems and charges on their structure. Staining CAM with fluorescent dyes is interesting in order to trace them, both by UV–vis absorption and fluorescence spectroscopies, in systems they are inoculated in. In particular, it may be advantageous when CAM are included in food formulations for animals, so that its erosion and transit kinetics in the intestine can be monitored. Techniques to increase the retention of hydrophilic molecules in CAM, and thus to control the release profiles, include coating the CAM with a polycation, so that a membrane can be formed on the CAM surface [27,34,37]. Chitosan (CS) is a good candidate for such purposes, since it is a hydrophilic, linear polysaccharide, derived from the natural polymer chitin, composed of randomly distributed β-(1-4) D-glucosamine and *N*-acetyl-glucosamine, thus showing positive charges below pH 6 [38]. In addition, it is a non-toxic, biodegradable, and highly mucoadhesive polymer [31,34,39]. CAM coated with CS have been reported in the literature [30,40].

In this paper, a new strategy to encapsulate hydrophilic, low molecular-weight, aromatic molecules in CAM is shown. It is based on the complexation of such molecules with a water-soluble polymer containing complementary charged aromatic rings. Complexation is due to aromatic–aromatic interactions between both aromatic, complementary charged molecules [14,16–18]. The method developed by our group provides binding forces strong enough to retain the dye in the CAM for a longer time. Both as a proof of concept, and for the special interest of staining CAM with robust methods that do not involve formation of covalent bonds, we choose R6G as the aromatic low molecular-weight model molecule, since it is cationic in a wide range of pH, presents high molar extinction coefficient so that is easily analyzed by UV–vis spectroscopy, and is fluorescent. The aromatic polyelectrolyte used for this study is poly(sodium 4-styrenesulfonate) (PSS), which is anionic in the whole range of pH. This polymer has shown to produce aromatic–aromatic interactions with several aromatic counterions, such as dyes [14–18], redox active molecules [41–44], and drugs [45]. As a negative control, we use poly(sodium vinylsulfonate) (PVS), a polyanion that does not bear aromatic rings. The release of the encapsulated complex is shown in both CAM and CAM coated with CS.

2. Experimental

2.1. Reagents

Commercially available PSS (Aldrich), PVS (Aldrich), CS (Novamatrix), ALG (EncapBioSystems), and R6G (Aldrich), were used as received to prepare solutions in deionized water. The structures of the different polyelectrolytes and R6G are shown in Fig. 2. The pH was adjusted with minimum amounts of NaOH and HCl. NaCl

(Merck) was used to adjust the ionic strength. Calcium chloride (Merck) was used for ALG gelation and CAM formation.

2.2. Equiment

The concentration of R6G was measured by UV–vis spectroscopy with a Heλios γ spectrophotometer. The pH was controlled on a UB10 DENVER instruments or CORNING Scholar 425 pH meters. The microencapsulation of R6G was performed with a four generation BIOTECH microencapsulator. A LEICA DM 2500 microscope was used to obtain visible and fluorescence images of the microcapsules. A thermoregulated SHEL LAB bath was used to maintain the temperature at constant values.

2.3. Procedures

Conventional procedures have been followed, and specific details are given in the captions to Figs. 3, 4 and 7–10. The concentration of the polymers is given in mol of monomeric units per liter. *R6G/PVS and R6G/PSS complex formation.* R6G/polyelectrolyte complexation was performed by mixing both components in water. The pH of the solutions was adjusted to 5. In order to ensure the complexes to fluoresce, the concentration of the polyelectrolyte was set to be 100-fold that of the dye. Complexes have been formed both at the feed concentration and at the maximum final concentration of the dye after encapsulation, and in the absence and in the presence of $CaCl_2$ 0.1 M. *CAM formation.* A volume of 7.4 mL of $7.5 \cdot 10^{-2}$ M ALG solution in water at pH 5 was injected through a syringe in the microencapsulator. Microencapsulation was performed using a nozzle of 200 μm of diameter, at a frequency of 940 Hz, under a flow rate of 4.4 mL/min, at 20 °C. The rain drops, product of the vibration of the instrument, were collected in a flask containing 200 mL of 0.1 M $CaCl_2$. CAM containing

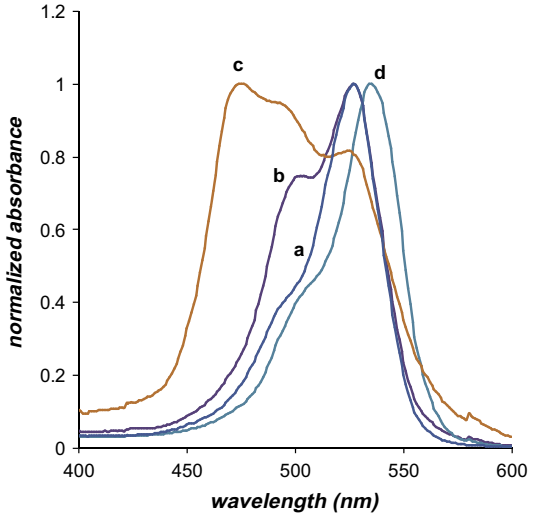

Fig. 3. Normalized UV–vis spectra of (a) R6G $1 \cdot 10^{-5}$ M; (b) R6G $1 \cdot 10^{-4}$ M; (c) R6G $1 \cdot 10^{-4}$ M in the presence de PVS $1 \cdot 10^{-2}$ M; (d) R6G $1 \cdot 10^{-4}$ M in the presence de PSS $1 \cdot 10^{-2}$ M.

R6G were prepared by the same method and including R6G at a concentration of 10^{-4} M, in the absence and in the presence of PVS (10^{-2} M) or PSS (10^{-2} M). After equilibrating for 30 min at 20 °C, the CAM were filtered, and the concentration of R6G in the supernatant was measured using UV–vis spectrophotometry, in order to calculate by subtraction from the total initial dye content the amount of dye encapsulated. Analyses were performed using quartz vessels with path lengths of 0.1–1 cm following conventional procedures in order to obtain absorbances lower than 1. Calibration curves were obtained both in the absence and in the presence of PSS and/or NaCl and/or $CaCl_2$, and are shown in Table 1.

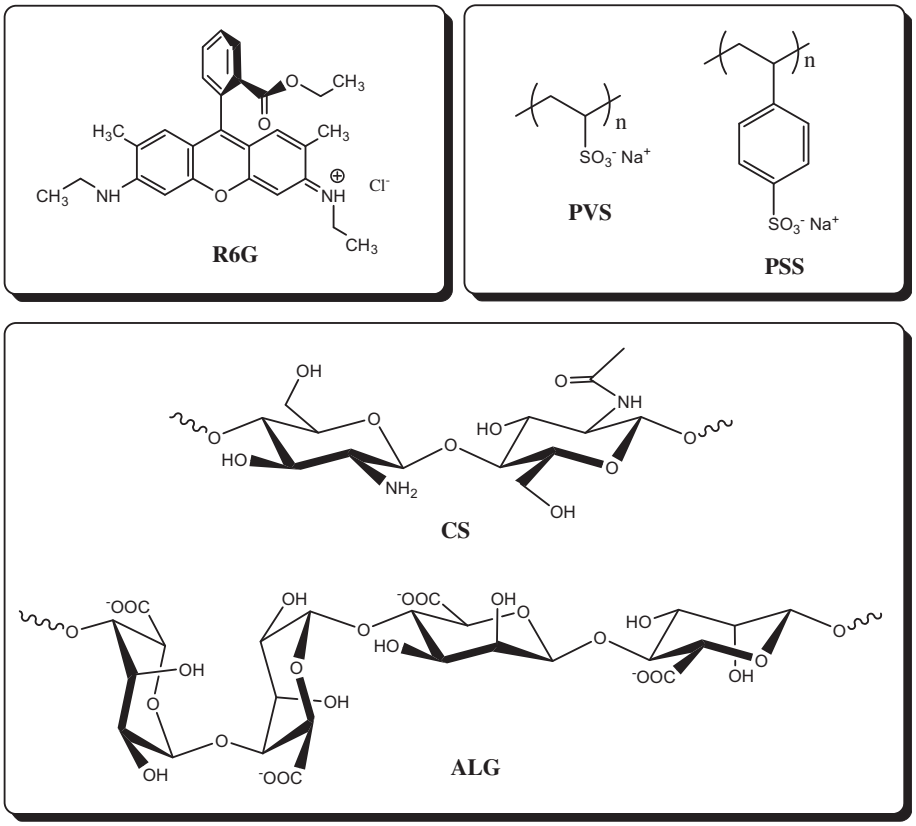

Fig. 2. Molecular structures.

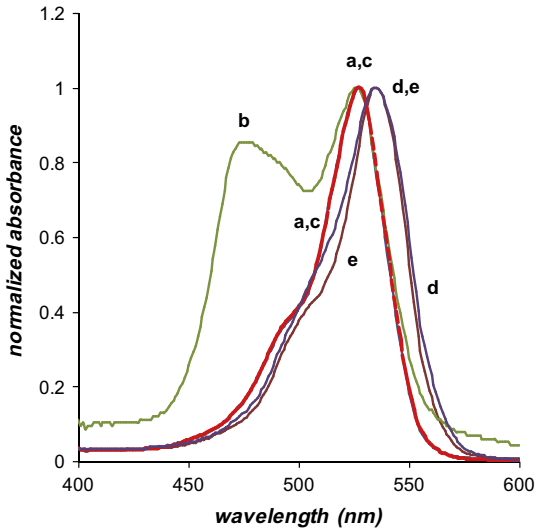

Fig. 4. Normalized UV–vis spectra of a $3.7 \cdot 10^{-6}$ M R6G solution in the absence of any additive (a), and in the presence of PVS $3.7 \cdot 10^{-4}$ M (b), PVS $3.7 \cdot 10^{-4}$ M and $CaCl_2$ 0.1 M (c), PSS $3.7 \cdot 10^{-4}$ M (d), and PSS $3.7 \cdot 10^{-4}$ M and $CaCl_2$ 0.1 M (e).

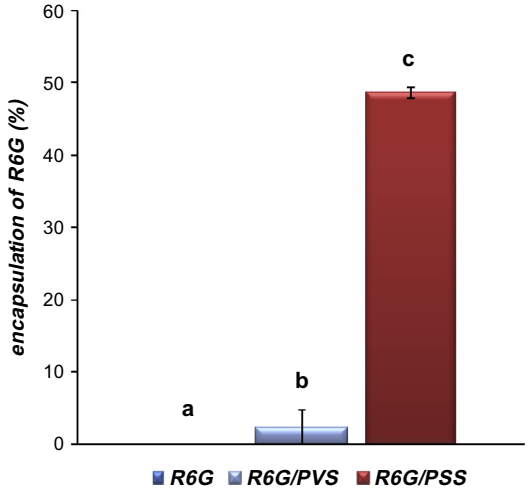

Fig. 5. Encapsulation of R6G in CAM in the absence of any sulfonated polyelectrolyte (a) and in the presence of PVS (b) or PSS (c).

R6G release studies from CAM. Once the microcapsules were formed and filtered, they were quickly washed with 10 mL of water at pH 5, and then incubated in 50 mL of 0.1 M NaCl aqueous solution adjusted to pH 5, or alternatively at pH 2, 3, 4, 6, 7, and 8, when the influence of the pH was studied. The concentration of R6G released from the CAM was evaluated at definite time intervals, by analyzing by UV–vis spectroscopy an aliquot of 2 mL which was poured back into the solution containing the microcapsules after measuring in order not to change the total volume. The experiments were conducted at temperatures of 7, 20, 30, and 60 °C. *CAM coating*. Once the microcapsules were formed and filtered, they were quickly washed with 10 mL of water at pH 5, and then incubated for 12 h in 50 mL of solutions containing CS at different concentrations at pH 5. Then, the CAM coated with CS (CS-CAM) were filtered and washed with 10 mL of water at pH 5. *R6G release studies from CS-CAM*. The CS-CAM were incubated in 50 mL of NaCl 0.1 M aqueous solution, at pH 2, 3, 4, and 5. The temperature was kept at 30 °C for 7 h, and the concentration of R6G released was evaluated as described before.

3. Results and discussion

3.1. Binding of R6G to different polyelectrolytes

The binding of cationic aromatic molecules such as R6G to different polyelectrolytes has been described previously [14,46]. Typical polyelectrolytes produce long-range electrostatic interactions with the dye, and, as a consequence of the increase on the local concentration of the dye around the polymer, the dyes tend to self-aggregate in a cooperative manner, forming aggregates of higher-order. However, if the polyelectrolyte bears complementary charged aromatic groups, aromatic–aromatic interactions are held between the dye and the polymeric aromatic rings, so that the dyes bind to the polyelectrolyte randomly distributed. Moreover, the first mechanism produces interactions that are easily cleaved in the presence of a high concentration of other electrolytes, since the long-range electrostatic interactions can be screened. On the contrary, aromatic–aromatic interactions are stronger [16–18,45] and do not cleave so easily in the presence of other electrolytes. These two mechanisms have an influence on the state of aggregation of the dye, which is easily followed by UV–vis spectroscopy.

It can be seen in Fig. 3 the normalized spectra of R6G in water at different experimental conditions. Monomeric R6G is found for the pristine dye at concentrations lower than 10^{-5} M (Fig. 3a). The corresponding spectrum shows a band centered at 527 nm, with a shoulder at 500 nm. At increasing concentrations, the band at 500 nm increases at the expense of that at 527 nm, as can be seen in Fig. 3b corresponding to a 10^{-4} M R6G solution in water, related to a higher probability to form dimers. In the presence of 100-fold the polyanion PVS, which does not bear aromatic groups, a 10^{-4} M R6G solution in water presents several bands at higher energies, revealing the formation of higher-order aggregates on the polymer environment, as can be seen in Fig. 3c. On the contrary, in the presence of 100-fold the polyanion PSS, which does bear aromatic groups to which the negative charge is attached, the corresponding spectrum shows the same profile as that of the monomeric R6G, but shifted 8 nm to lower energies, as can be seen in Fig. 3d. This is due to the interaction between the dipole moments of the closely interacting aromatic moieties by aromatic–aromatic interactions of both the polymer and the dye. Solutions containing 10^{-4} M of R6G in the absence and in the presence of 100-fold these two polyelectrolytes have been used to prepare the CAM.

According to the experimental procedure, 7.4 mL of the concentrated sodium alginate solution containing R6G and/or other polymers is poured into 200 mL of a highly concentrated $CaCl_2$ aqueous solution. Thus, if none of the added R6G is encapsulated in the formed CAM, its concentration should be reduced to $3.7 \cdot 10^{-6}$ M. In Fig. 4, the normalized spectra of R6G corresponding to this dilute condition, in the absence and in the presence of 0.1 M $CaCl_2$ and/or the different sulfonated polyelectrolytes are shown. Note that in the presence of PVS, higher-order aggregates are still formed (Fig. 4b), which are, however, cleaved in the presence of $CaCl_2$, as can be seen in Fig. 4c, conditions at which a spectrum equivalent to that of the pristine R6G, represented in Fig. 4a, is found. In contrast, the spectra in the presence of 100-fold PSS, independently on the $CaCl_2$ concentration (Figs. 4d and 4e), present their maxima shifted to lower energies, confirming that the R6G/PSS complex is not cleaved even at high ionic strength conditions. These findings are important, since they allow us anticipating that the encapsulation of R6G in the presence of PVS may not differ much from the encapsulation of the pristine dye, since the possible complex with PVS is cleaved in the presence of the calcium salt. On the contrary, as hypothesized, PSS may be able to produce a different pattern of R6G encapsulation, since the R6G/PSS complex is stable at the strong cleaving conditions of the encapsulation procedure.

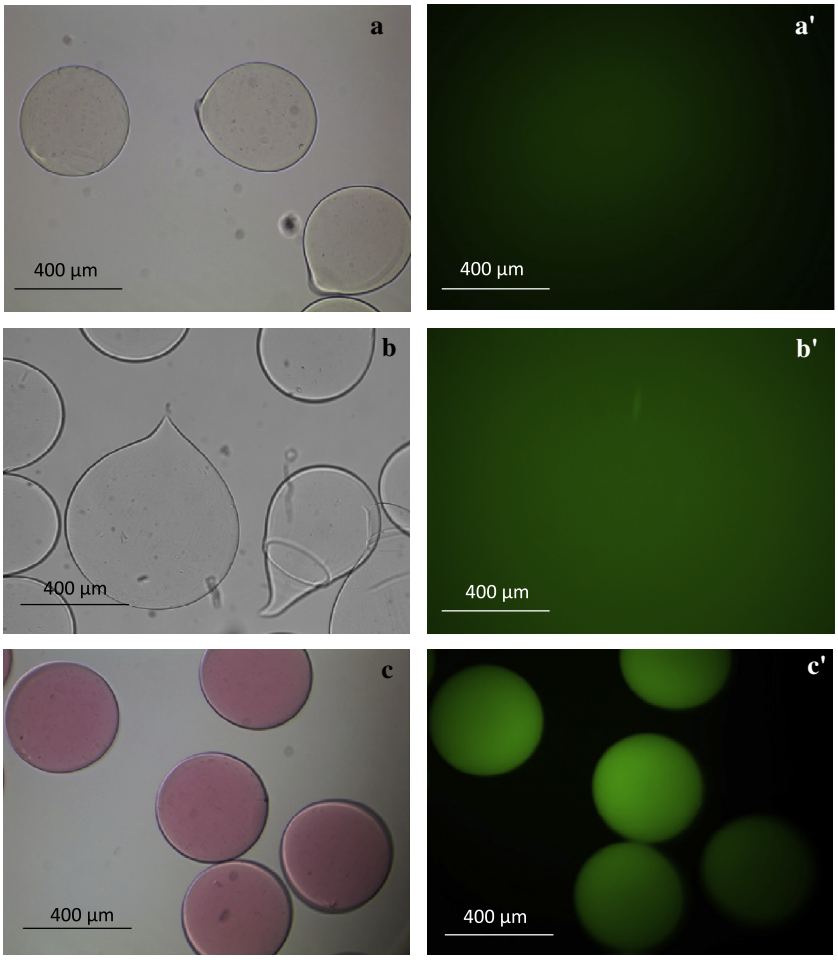

Fig. 6. Optical (left) and fluorescence (right) microscopy images of CAM immersed in the reaction medium and formed by incorporation in the reactive ALG solution R6G in the absence of any sulfonated polyelectrolyte (a, a′), and in the presence of PVS (b, b′) or PSS (c, c′).

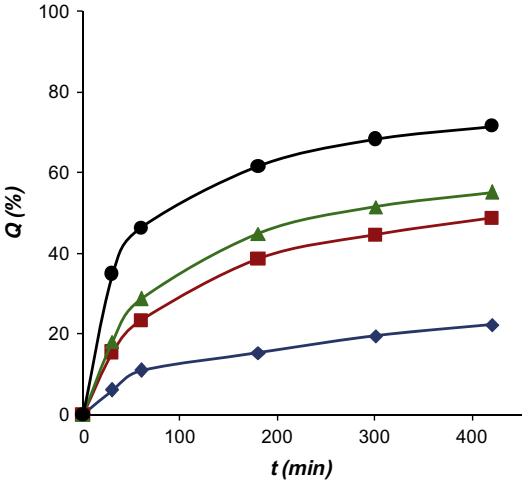

Fig. 7. Cumulative release (*Q*%) of the R6G/PSS complex from CAM incubated in 0.1 M NaCl aqueous solution as a function of *t* at different temperatures: (♦) 7 °C; (■) 20 °C; (▲) 30 °C; (●) 60 °C.

3.2. Encapsulation of R6G in CAM

After preparing the CAM in the presence of R6G and/or PVS or PSS, and equilibrating for 30 min, the concentration of R6G encapsulated in the CAM was calculated by analyzing the R6G present in the supernatant. As expected, no encapsulation of R6G was achieved when CAM where prepared in the absence of PSS, as can be seen in Fig. 5. Note that ALG, as PVS, is also a polyanion, susceptible of interaction with R6G by long-range electrostatic interactions. However, the high ionic strength furnished by the $CaCl_2$ screens the corresponding interaction in the case of PVS, and, in the case of ALG, in addition to the screening effect, the strong binding of Ca^{2+} to the polysaccharide minimizes the interaction with R6G. In summary, both polyelectrolytes that do not bear aromatic rings lose the ability to retain the dye on their environment, and as a consequence of this, the dye rapidly diffuse out of the CAM. On the contrary, the stability of the R6G/PSS complex allows around a 50% of the dye to be retained inside the CAM, since the large size of the complex produces stronger interactions with the CAM matrix, and thus a slower diffusion from the microcapsules [26,31]. Moreover, the R6G released from the CAM is not found as free dye, but complexed with PSS, as observed in the analysis of the supernatant, that showed the R6G UV–vis band shifted 4 nm to lower energies. Thus, in fact, the species that is released from the CAM is the R6G/PSS complex itself.

Optical microscopy, as well as fluorescence microscopy, clearly illustrates the adjuvant role of PSS on the encapsulation of the aromatic low molecular-weight dye. As can be seen in Fig. 6, in the absence of any added polyelectrolyte or in the presence of PVS, the microcapsules do not show significant encapsulation of the dye, and they are not differentiated from the bulk in the fluorescence microscopy image, indicating that the dye is dispersed in the bulk. On the contrary, when fabricated including the R6G/PSS

Table 1
Calibration curves obtained at 20 °C and pH 5 for R6G solutions at different conditions; y is the absorbance at 527 nm; x is the R6G concentration in M, and R^2 is the linear regression factor.

R6G concentration range (M)	PSS concentration (M)	NaCl concentration (M)	$CaCl_2$ concentration (M)	Calibration curve	R^2
$1 \cdot 10^{-6}$–$1 \cdot 10^{-5}$	–	–	–	$y = 72729x - 0.0173$	0.9994
$1 \cdot 10^{-6}$–$1 \cdot 10^{-5}$	–	–	0.1	$y = 78841x + 0.0065$	0.9993
$1 \cdot 10^{-6}$–$1 \cdot 10^{-5}$	$3.7 \cdot 10^{-4}$	–	–	$y = 68795x + 0.0026$	0.9981
$1 \cdot 10^{-6}$–$1 \cdot 10^{-5}$	$3.7 \cdot 10^{-4}$	0.1	–	$y = 53915x + 0.0156$	0.9970
$1 \cdot 10^{-6}$–$1 \cdot 10^{-5}$	$3.7 \cdot 10^{-4}$	–	0.1	$y = 50959x + 0.0127$	0.9984

complex, it is clearly observed a strong pink color in the CAM, whilst highly contrasted images are obtained in the fluorescence picture. Note that, independently of the high local concentration of the dye, the large excess of PSS produces dispersion of R6G along the polymer chain in the complexes avoiding the dye self-aggregation and the consequent fluorescence quenching; thus the stained material shows fluorescence.

3.3. Release of the R6G/PSS complex from CAM

The CAM containing the R6G/PSS complex were filtered from the $CaCl_2$ solution, and then incubated in different media. Preliminary experiments performed at pH 5 show that the dye is faster released in the presence of high concentrations of NaCl. This faster release may be due, in addition to swelling of the microcapsules [33], to ion exchange between Na^+ and Ca^{2+}, which may break the egg box conformation [47], so that the free carboxylic groups undergo electrostatic repulsion facilitating the CAM erosion and gradual process of disintegration [29,48]. However, disintegration was not observed at the time scale of our experiments. In addition, the uptake of Na^+ and Cl^- ions by the CAM can also increase the osmotic strength, therefore increasing the pore size, favoring the release of the R6G/PSS complex.

In consequence, and in order to obtain relatively fast release profiles, the release of the R6G/PSS complex at different temperatures has been studied in the presence of 0.1 M NaCl, and the results are plotted in Fig. 7. It can be observed that with the increase on the temperature the rate of release of the complex increases. Several methods have been reported in the literature to explain and quantitatively calculate the diffusion constants of polymers in different media [49–55]. Although contrasting the different models is beyond the purpose of this paper, some insights can be given that allow understanding the behavior of the system. The release of the complex follows a pattern derived for transport of molecules such as drugs in swellable spherical matrices, characterized by the Peppas equation

$$Q = Kt^{0.43} \quad (1)$$

where Q is the cumulative dye molar fraction released in percentage, K is a constant incorporating characteristics of the macromolecular network, and t is time. This can be seen in Fig. 8, where Q values lower than 50% have been considered. The corresponding K values are listed in Table 2. The fit parameter 0.43 is related, as said before, to a release mechanism controlled by diffusion in spherical matrices [50]. Note that the CAM are hydrated at $t = 0$, so that swelling and consequent relaxation of the ALG chains do not appear to contribute significantly in this case. Moreover, the overall negative charge of the R6G/PSS complex produces repulsive interactions with the negatively charged ALG chains, avoiding attractive electrostatic interactions with the ALG network. The increase on the temperature may, among other effects on the polymer matrix, increase the diffusion coefficient of the complex, facilitating its release from the CAM.

Variations on release profiles of encapsulated molecules with the pH have been described in the literature [26,28–29,31,33].

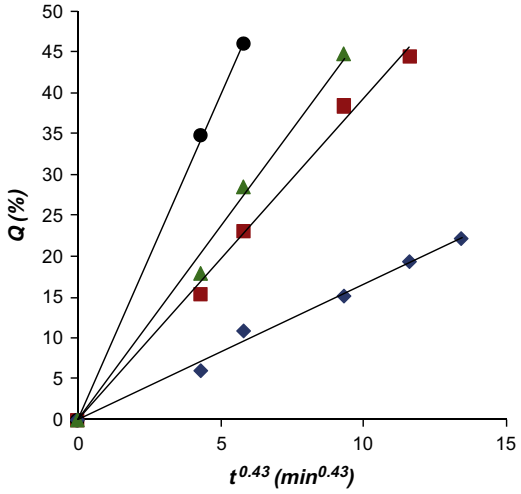

Fig. 8. Cumulative release (Q%) of the R6G/PSS complex from CAM incubated in 0.1 M NaCl aqueous solution as a function of $t^{0.43}$ at different temperatures: (♦) 7 °C; (■) 20 °C; (▲) 30 °C; (●) 60 °C.

Table 2
Peppas' constants (K) and linear regression factors (R^2) for the release of R6G/PSS complex from CAM as a function of the temperature (T).

T (K)	K ($min^{-0.43}$)	R^2
280	1.659	0.991
293	3.924	0.994
303	4.742	0.992
333	7.978	0.999

These variations are related to changes in the CAM structure upon shifting the acid-base equilibrium of the carboxylic groups interplaying with the effect of the ionic strength. However, in our systems, the pH does not seem to have a definite influence on the release profiles of the R6G/PSS complex, when varied at 30 °C in the presence of 0.1 M NaCl in a range of pH from 2 to 8, as can be seen in Fig. 9.

3.4. Release of the R6G/PSS complex from CS-CAM

In order to improve the retention of the R6G/PSS complex inside the CAM, these were coated with CS by incubating the CAM in CS solutions at different concentrations. Murata et al. [27] reported a higher retention of brilliant blue when the CAM were incubated in increasingly concentrated CS solutions. CS is considered to form a membrane on the CAM surface by electrostatic complexation between CS and ALG [30,38–40] preventing its swelling, erosion and disintegration [29], as well as the passage of different ions and molecules, as it could be the case of the R6G/PSS complex. Li et al. [39] reported that the better condition for the structuration of CS membranes around CAM is pH 5, forming denser membranes than at lower or higher pH, explained invoking that approximately

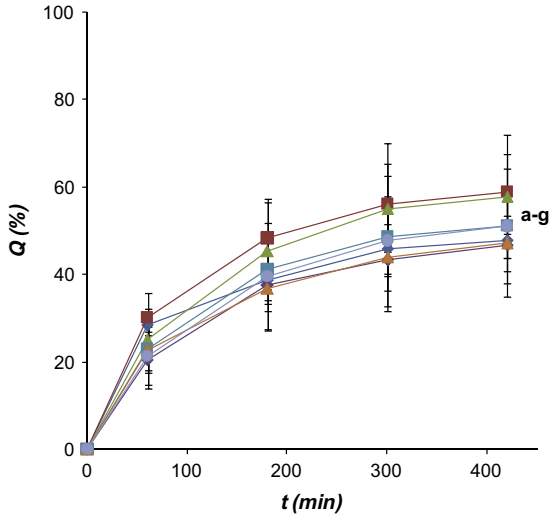

Fig. 9. Cumulative release (Q%) of the R6G/PSS complex from CAM incubated in 0.1 M NaCl aqueous solution at 30 °C as a function of *t* at pH 2 (a), 3 (b), 4 (c), 5 (d), 6 (e), 7 (f), and 8 (g).

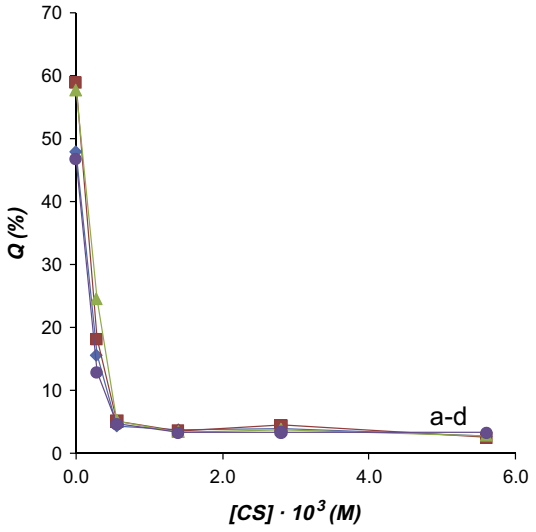

Fig. 10. Cumulative release (Q%) of the R6G/PSS complex from CS-CAM incubated in 0.1 M NaCl aqueous solution at 30 °C after 420 min as a function of the original CS concentration in incubation medium at pH 2 (a), 3 (b), 4 (c), and 5 (d).

the 70 – 80% of the amine and carboxylic groups are charged, therefore, each polysaccharide presenting a linear, rigid conformation [30,38,40]. Gaserod et al. [40] reported higher resistance of CS-CAM to disintegration in highly concentrated saline solutions, which appeared to directly correlate to the amount of CS used.

Accordingly to the above exposed, CAM were coated with CS at pH 5. The release of the R6G/PSS complex from CS-CAM was then evaluated in the presence of 0.1 M NaCl at 30 °C in a range of pH between 2 and 5. The pH was not taken to higher values in order to ensure protonation of CS. The coated microcapsules show significantly greater retention of the R6G/PSS complex after 420 min compared with uncoated microcapsules, as can be seen in Fig. 10. Note that the presence of increasing concentrations of CS produces a decrease on the amount of complex released, achieving nearly negligible values (lower than 5%) at a CS concentration of $5.6 \cdot 10^{-4}$ M or higher. At very low concentration of CS in the coating solution (concentrations one order of magnitude lower than the apparent ALG concentration) the lower retention shown could be due to the formation of an incomplete membrane.

4. Conclusions

A new strategy to encapsulate hydrophilic, low molecular-weight, aromatic molecules, such as R6G, in CAM has been shown. The encapsulation strategy is based on the complexation of the aromatic molecule with an aromatic polyelectrolyte, such as PSS. PSS and R6G form a complex based on aromatic–aromatic interactions, which are strong enough to resist the cleaving effect of the conditions of the CAM formation reaction medium. On the contrary, direct immobilization of the dye resulted unsuccessful due to its high diffusion coefficient in the aqueous medium, and complexation with the non-aromatic polyelectrolyte PVS did not improve the immobilization, since the corresponding complex is based on long-range electrostatic interactions, which are easily cleaved under the high ionic strength conditions of the microcapsule formation reaction. The large size of the R6G/PSS complex produces immobilization of the dye in the microcapsules. Besides, the diffusion of the complex can be controlled by coating the CAM with CS, and may be practically prevented in the presence of relatively low CS concentration. The release of the R6G/PSS complex from the CAM is dependent on the temperature, but does not depend on the pH, at the ranges studied in this work. Apart from the interest on staining CAM, the results shown here represent a proof of concept of the potential use of aromatic–aromatic interactions in improving materials performance and controlling interesting physicochemical properties.

Acknowledgments

The authors thank FONDECYT (Grants Nos. 1090341, 1120514, and 11121481) and Innova-CORFO (Grant No. 07-CN-13-PPT-256) for financial support.

References

[1] V. Martínez Martínez, F. López Arbeloa, J. Bañuelos Prieto, I. López Arbeloa, J. Phys. Chem. B 109 (2005) 7443–7450.
[2] D. Avnir, D. Levy, R. Reisfeld, J. Phys. Chem. 88 (1984) 5956–5959.
[3] P.D.G. Dean, D.H. Watson, J. Chromatogr. A 165 (1979) 301–319.
[4] S.-H. Kim, S.-M. Lee, D.-U. Kim, J.-Z. Cui, S.-W. Kang, Dyes Pigm. 49 (2001) 103–108.
[5] G. Li, J. Xiao, W. Zhang, Dyes Pigm. 92 (2012) 1091–1099.
[6] J.H. Wang, J.D. Bartlett, A.C. Dunn, S. Small, S.L. Willis, M.J. Driver, A.L. Lewis, J. Microsc. 217 (2005) 216–224.
[7] F.L. Arbeloa, M.T. Estevez, T.L. Arbeloa, I.L. Arbeloa, Clay Miner. 32 (1997) 97–106.
[8] G. Payne, B. Reedy, C. Lennard, B. Comber, D. Exline, C. Roux, Forensic Sci. Int. 150 (2005) 33–51.
[9] V. Martínez Martínez, F. López Arbeloa, J. Bañuelos Prieto, T. Arbeloa López, I. López Arbeloa, J. Phys. Chem. B 108 (2004) 20030–20037.
[10] G.S. Manning, Q. Rev. Biophys. 11 (1978) 179–246.
[11] G.S. Manning, J. Phys. Chem. 88 (1984) 6654–6661.
[12] E. Nordmeier, Macromol. Chem. Phys. 196 (1995) 1321–1374.
[13] M.H. Hao, S.C. Harvey, Macromolecules 25 (1992) 2200–2208.
[14] I. Moreno-Villoslada, J.P. Fuenzalida, G. Tripailaf, R. Araya-Hermosilla, G.d.C. Pizarro, O.G. Marambio, H. Nishide, J. Phys. Chem. B 114 (2010) 11983–11992.
[15] I. Moreno-Villoslada, C.S. Torres-Gallegos, R. Araya-Hermosilla, H. Nishide, J. Phys. Chem. B 114 (2010) 4151–4158.
[16] I. Moreno-Villoslada, F. González, L. Arias, J.M. Villatoro, R. Ugarte, S. Hess, H. Nishide, Dyes Pigm. 82 (2009) 401–408.
[17] I. Moreno-Villoslada, R. González, S. Hess, B.L. Rivas, T. Shibue, H. Nishide, J. Phys. Chem. B 110 (2006) 21576–21581.
[18] I. Moreno-Villoslada, M. Jofré, V. Miranda, R. González, T. Sotelo, S. Hess, B.L. Rivas, J. Phys. Chem. B 110 (2006) (1812) 11809–11812.
[19] A. Tanriseven, Ş. Doğan, Process Biochem. 36 (2001) 1081–1083.
[20] A. Blandino, M. Macıas, D. Cantero, Proc. Biochem. 36 (2001) 601–606.
[21] Y. Chai, L.H. Mei, G.L. Wu, D.Q. Lin, S.J. Yao, Biotechnol. Bioeng. 87 (2004) 228–233.
[22] R.J. Mumper, A.S. Huffman, P.A. Puolakkainen, L.S. Bouchard, W.R. Gombotz, J. Controlled Release 30 (1994) 241–251.
[23] K.I. Draget, G. Skjåk-Bræk, O. Smidsrød, Int. J. Biol. Macromol. 21 (1997) 47–55.
[24] A.C. Hodsdon, J.R. Mitchell, M.C. Davies, C.D. Melia, J. Control. Release 33 (1995) 143–152.
[25] J. Tu, S. Bolla, J. Barr, J. Miedema, X. Li, B. Jasti, Int. J. Pharm. 303 (2005) 171–181.

[26] A. Kikuchi, M. Kawabuchi, A. Watanabe, M. Sugihara, Y. Sakurai, T. Okano, J. Control. Release 58 (1999) 21–28.
[27] Y. Murata, T. Maeda, E. Miyamoto, S. Kawashima, Int. J. Pharm. 96 (1993) 139–145.
[28] W.R. Gombotz, S. Wee, Adv. Drug Deliv. Rev. 31 (1998) 267–285.
[29] A. Kikuchi, M. Kawabuchi, M. Sugihara, Y. Sakurai, T. Okano, J. Control. Release 47 (1997) 21–29.
[30] O. Gåserød, O. Smidsrød, G. Skjåk-Bræk, Biomaterials 19 (1998) 1815–1825.
[31] M. George, T.E. Abraham, J. Control. Release 114 (2006) 1–14.
[32] A.F. Stockwell, S.S. Davis, S.E. Walker, J. Control. Release 3 (1986) 167–175.
[33] H.H. Tonnesen, J. Karlsen, Drug Dev. Ind. Pharm. 28 (2002) 621–630.
[34] P.R. Hari, T. Chandy, C.P. Sharma, J. Appl. Polym. Sci. 59 (1996) 1795–1801.
[35] E. Taqieddin, M. Amiji, Biomaterials 25 (2004) 1937–1945.
[36] T.L. Lemke, D.A. Williams, Foye's Principles of Medicinal Chemistry, Wolters Kluwer Health, 2012.
[37] M.L. Huguet, E. Dellacherie, Process Biochem. 31 (1996) 745–751.
[38] K.Y. Lee, W.H. Park, W.S. Ha, J. Appl. Polym. Sci. 63 (1997) 425–432.
[39] X.-Y. Li, L.-J. Jin, T.A. McAllister, K. Stanford, J.-Y. Xu, Y.-N. Lu, Y.-H. Zhen, Y.-X. Sun, Y.-P. Xu, J. Agric. Food Chem. 55 (2007) 2911–2917.
[40] O. Gaserod, A. Sannes, G. Skjak-Braek, Biomaterials 20 (1999) 773–783.
[41] I. Moreno-Villoslada, V. Miranda, R. Gutiérrez, S. Hess, C. Muñoz, B.L. Rivas, J. Membr. Sci. 244 (2004) 205–213.
[42] I. Moreno-Villoslada, F. González, L. Rivera, S. Hess, B.L. Rivas, T. Shibue, H. Nishide, J. Phys. Chem. B 111 (2007) 6146–6150.
[43] I. Moreno-Villoslada, M. Soto, F. Gonzalez, F. Montero-Silva, S. Hess, I. Takemura, K. Oyaizu, H. Nishide, J. Phys. Chem. B 112 (2008) 5350–5354.
[44] I. Moreno-Villoslada, C. Torres, F. González, M. Soto, H. Nishide, J. Phys. Chem. B 112 (2008) 11244–11249.
[45] I. Moreno-Villoslada, F. Oyarzún, V. Miranda, S. Hess, B.L. Rivas, Polymer 46 (2005) 7240–7245.
[46] I. Moreno-Villoslada, C. Torres-Gallegos, R. Araya-Hermosilla, J.P. Fuenzalida, O.G. Marambio, G.d.C. Pizarro, M.E. Flores, T. Murakami, H. Nishide, Mol. Cryst. Liq. Cryst. 522 (2010) 136/[436]–147/[447].
[47] S.K. Bajpai, S. Sharma, React. Funct. Polym. 59 (2004) 129–140.
[48] X. Wang, H. Garth Spencer, Polymer 39 (1998) 2759–2764.
[49] L. Masaro, X.X. Zhu, Prog. Polym. Sci. 24 (1999) 731–775.
[50] J. Siepmann, N.A. Peppas, Adv. Drug Deliv. Rev. 48 (2001) 139–157.
[51] J. Siepmann, N.A. Peppas, Int. J. Pharm. 418 (2011) 6–12.
[52] M. Olukman, O. Şanlı, E.K. Solak, J. Biomater. Nanobiotechnol. 3 (2012) 469–479.
[53] S. Dash, P.N. Murthy, L. Nath, P. Chowdhury, Acta Pol. Pharm. 67 (2010) 217–223.
[54] M.H. Shoaib, J. Tazeen, H.A. Merchant, R.I. Yousuf, Pakistan J. Pharm. Sci. 19 (2006) 119–124.
[55] P. Gao, P. Fagerness, Pharm. Res. 12 (1995) 955–964.